Journal of Physics:
Conference Series

PURPOSE-LED PUBLISHING™

PAPER • **OPEN ACCESS**

Virtual development of a multi-cylinder hydrogen spark ignition engine operating at lean burn conditions

To cite this article: Emanuele Ugliano *et al* 2024 *J. Phys.: Conf. Ser.* **2893** 012100

View the article online for updates and enhancements.

You may also like

- Knock detection in spark ignition engines using a nonlinear wavelet transform of the engine cylinder head vibration signal
Ning Li, Jianguo Yang, Rui Zhou et al.
- The study of the spark ignition engine performance at fueling with n-butanol-gasoline mixture
Cr Sandu, C Pana, N Negurescu et al.
- Determination of knock characteristics in spark ignition engines: an approach based on ensemble empirical mode decomposition
Ning Li, Jianguo Yang, Rui Zhou et al.

This content was downloaded from IP address 143.225.115.253 on 09/12/2024 at 09:02

Journal of Physics: Conference Series **2893** (2024) 012100 doi:10.1088/1742-6596/2893/1/012100

Virtual development of a multi-cylinder hydrogen spark ignition engine operating at lean burn conditions

Emanuele Ugliano[1*], Fabio Bozza[1], Luigi Teodosio[1],

1. Industrial Engineering Department, Via Claudio n.21, University of Naples, Federico II, Napoli, Italy;

*Corresponding author: emanuele.ugliano@unina.it

Abstract. Propulsion systems for automotive applications are facing the issues related to the stringent noxious emission and CO_2 regulations which are driving the manufacturer and the researchers to the development of innovative powertrains. Among the different solutions, relevant efforts are being directed towards the decarbonisation of internal combustion engines (ICEs). In this scenario, the hydrogen, particularly the green one obtained through the water electrolysis using renewable energy sources, is emerging as a promising fuel for a future sustainable mobility. In this work, a multi-cylinder hydrogen Spark Ignition (SI) engine conceived for automotive applications is developed and optimized to operate under ultra/lean air/hydrogen mixtures. In particular, a 3-cylinder turbocharged hydrogen SI engine is virtually developed through a 0D/1D model, starting from a naturally aspirated single-cylinder SI unit; the latter is properly validated with experiments and 3D CFD outcomes in a previous authors' activity. A fractal model is used for combustion modelling, coupled to a user-defined turbulence sub-model. The thermo-diffusive instability sub-model, based on Howarth theory, is integrated into the combustion model to correctly simulate the hydrogen engine operation at ultra/lean mixtures. In addition, the knock onset is evaluated with a Tabulated Kinetic of Ignition (TKI) approach, requiring a pre-computation of the auto-ignition delay times at varying the thermodynamic conditions. The main aim of the work is to forecast the hydrogen engine operation under full load and ultra-lean conditions, analysing performance, efficiency and NOx emissions at the knock limit. Subsequently, an optimization of the engine operation is carried out exploring different compression ratios, air/fuel proportions (lambda values) and water-to-fuel ratios. The objective of the initial optimisation is to optimise efficiency while respecting the safety constraint on the occurrence of shocks. Comparison with the base case, in which the maximum value is 35.6%, reveals an increase of 1.98% with CR equal to 13. However, in the case of the high-speed analysis, there is a decrease compared to the base case. The second analysis shows that the maximum lambda value that meets the imposed BMEP target is 2.1, thus minimising the NOx emissions of a multi-cylinder hydrogen engine under all conditions. A final analysis was conducted to study the impact of water injection on NOx for fixed rpm.

1. Introduction

In the recent years, the transport sector has undergone a significant transformation due to its substantial contribution to greenhouse gas emissions and the restrictions imposed by the European Union on the pollutant emissions; different solutions are being explored in order to achieve the carbon neutrality. To this aim, there are a number of potential technical solutions, including the electrification of transport units or the utilisation of carbon-neutral fuels. From this perspective, hydrogen represents a particularly

Content from this work may be used under the terms of the Creative Commons Attribution 4.0 licence. Any further distribution of this work must maintain attribution to the author(s) and the title of the work, journal citation and DOI.
Published under licence by IOP Publishing Ltd

promising option being a carbon-free fuel and, therefore, contributing to mitigate the impact of CO_2 emissions on the global warming. Hydrogen presents additional benefits if compared to the conventional fuels. The lower heating value of the hydrogen is 120 MJ/kg, which is considerably higher than that of petrol, which is 43.4 MJ/kg. Furthermore, hydrogen has a high laminar flame speed and a broad flammability range, enabling its use with lean and ultra-lean mixtures to increase the thermal efficiency and to reduce the NOx emissions in internal combustion engines (ICEs) applications. Additionally, the high octane number of hydrogen contributes to its resistance to knock occurrence, allowing for the employment of increased geometrical compression ratios which, in turn, contributes to improve the engine efficiency [1]. However, hydrogen also presents a number of issues to be adequately addressed. The first of these concerns the prevention of the abnormal combustions (i.e. pre-ignition, backfiring), which are generated due to the wide flammability range and the low activation energy [2]. Furthermore, the low volumetric energy density of hydrogen compared to fossil fuels [3] is another negative aspect to be take into account. In order to mitigate these drawbacks, some techniques such as the direct injection configuration, the use of ultra-lean air/hydrogen mixtures can be employed to reduce the phenomena of abnormal combustion, including the knock. Another technique that could bring benefits in terms of both knock mitigation and reduction in NOx is the liquid water injection, which reduces the in-cylinder temperatures of unburned mixture [4],[5]. In the existing literature, there are several experimental and numerical papers discussing the performance of the hydrogen SI engines at the development and design stage. Most of the literature works based on the numerical approach employ three-dimensional CFD techniques. For instance, the study conducted by Maio G. at al. [6] investigated with experiments and 3D modelling the performance of a heavy-duty hydrogen engine at fixed speed exploring two distinct injection configurations, namely port fuel injection (PFI) and direct injection (DI). CFD model successfully simulates different engine operating conditions for both PFI and DI systems. It demonstrated that the charge stratification induced by DI system increased the wall heat losses and the NOx formation. Luo Y. et al. [7] examined the impact of the start of injection (SOI) on the combustion development, thermal efficiency and NOx emissions of a 1.5L turbocharged DI hydrogen engine using both experimental and 3D CFD approaches. This study proposes some control strategies to realize lean and efficient combustion in hydrogen SI engine, mainly focusing on the effects of the combustion chamber shape and injection strategy on the hydrogen mixing.
Also some authors of present work analysed in [8] the performance of a single-cylinder turbocharged hydrogen SI engine for marine applications, employing a 1D/3D numerical methodology. They investigated the advantages of the ultra-lean hydrogen combustion in terms of efficiency and thermal NO for limited medium/high load points.
The analysis of literature papers highlights the lack of a robust numerical procedure to develop and optimize with low computational cost a multi-cylinder hydrogen SI engine operating under ultra-lean hydrogen/air mixtures.
To overcome this lack in the current technical literature, the objective of this work is to show how a 0D/1D model using phenomenological models can be used to predict the performance of a multi-cylinder hydrogen engine in terms of power and emissions, providing insights that can be used in engine design. the study also analyses the effects of compression ratio, λ level and water injection on the engine performance at full load, trying to provide a guideline for the development of hydrogen SI engines characterized by increased thermal efficiency and reduced NOx emissions to be employed in future small- to medium-size vehicles.

2. Engine system and experiments

The virtual engine model was developed on the basis of a single-cylinder naturally aspirated research engine, mounted on a steady test bench; the engine is equipped with a direct injection system, injecting the hydrogen at low pressure. The single-cylinder hydrogen unit was tested in different speeds and

equivalence ratios, collecting the main performance parameters and the in-cylinder pressure traces. The most important features of this engine can be seen in Table 1.

Table 1. Main engine characteristics.

Engine Model	Single-cylinder hydrogen unit
Compression ratio	10.0:1
Bore/Stroke, mm	87/85
Displaced volume, cm^3	505
Valve number	1 intake / 1 exhaust
Injection configuration	DI

3. Model description

This section provides a comprehensive overview of the 1D engine model used for the considered engine. The 1D engine model (GT-Power) is schematized as a network of intake/exhaust pipes connected to the cylinder through the valves and also including the direct fuel injector. 1D flow equations are solved for the pipes, while the cylinder is assumed as a single 0D volume with thermo-dynamic properties uniform over the element. During the combustion event, the cylinder volume is sub-divided into two zone (burned and unburned), solving the mass and energy conservation equations for each zone. Friction losses are modelled implementing an empirical correlation, computing the friction mean effective pressure (FMEP) as a function of mean piston speed and in-cylinder pressure peak.

A particular emphasis will be devoted to the description of advanced 0D sub-models aiming to reproduce the in-cylinder processes. The latter includes the turbulence, the hydrogen combustion with thermo-diffusive (TD) instability, the heat transfer, knock and NOx emissions.

3.1. In-cylinder sub-models

As mentioned above, the in-cylinder phenomena are modelled using in-house developed sub-models to correctly reproduce the turbulence, combustion, heat transfer, NOx emissions and knock. The flow and turbulence evolutions along the engine cycle are predicted by the K-k-T-S 0D turbulence sub-model [9],[10] based on four governing equations. This sub-model solves the mean flow kinetic energy, the turbulent kinetic energy, and the specific angular momentum of tumble and swirl motions. The combustion sub-model is a phenomenological model, based on the fractal theory, which considers the enhancement of the burning speed induced by the turbulence through an increase of the effective flame area (turbulent area) with respect to the laminar one, without interactions between turbulence field and chemical kinetics [11]. This approach allows for the evaluation of the burning rate according to the following equation (1):

$$\frac{dm_b}{dt} = \rho_u \cdot S_L \cdot A_L \cdot \Sigma \qquad (1)$$

where ρ_u is the unburned gas density, m_b is the burned mass, A_L the area of the laminar flame front and Σ is the wrinkling ratio; the latter accounts for the increased area of the turbulent flame front with respect to the laminar one, due to the turbulence. S_L is the laminar flame speed (LFS) and for the hydrogen fuel is calculated through a chemical-derived correlation presented in [12]; it represents a fitting of LFS chemical kinetic calculations performed adopting the scheme proposed by Zhang. To correctly characterise the combustion of hydrogen engines, especially those operating with ultra-lean mixtures, the Darrieus-Landau (DL) and thermo-diffusive (TD) instabilities have to be properly taken into account

within the combustion model; in this work, the TD sub-model based on the theory presented by Howarth et al. [13] is coupled to the combustion model as De Bellis et al. work [14]. The equation proposed by Howarth et al [13] is as follows:

$$S_F = \begin{cases} \exp(0.08w_2)\, S_L & if \quad p < \Pi_c \\ (1 + 0.47w_2) S_L & if \quad p > \Pi_c \end{cases} \tag{2}$$

$$\delta_F = \begin{cases} \exp(-0.06w_2)\, \delta_L & if \quad p < \Pi_c \\ \frac{\delta_L}{(1+0.26w_2)} & if \quad p > \Pi_c \end{cases} \tag{3}$$

$$\Pi_c = \left(\frac{20}{7 - 2\theta}\right)^{\frac{150}{20+10\theta}} \tag{4}$$

$$\theta = \frac{T}{300} \tag{5}$$

Where w_2 is a parameter that can correctly characterise the instability for lean mixtures [15], the subscript L defines those parameters that do not take TD effects into account, while the subscript F defines those that do have TD effects within them. While Π_c separates two regions where two different matchings have been proposed. Furthermore, Howarth theory adds to equations (2) and (3) other equations (4) and (5) to consider the interaction between TD and turbulence, through the Karlovitz number (Ka) where subscript S are the terms that consider this iteration

$$S_s = \left(1 + 0.26 \exp(-0.038w_2) \sqrt{K_a}\right) S_F \tag{6}$$

$$\delta_s = \frac{\delta_F}{\left(1 + 0.22 \exp(-0.026w_2) \sqrt{K_a}\right)} \tag{7}$$

In this case, the TD instability model increases the overall burning rate according to a characteristic instability parameter affected by the engine thermodynamic conditions (pressure and temperature) and the equivalence ratio. (The knock process is simulated using the tabulated kinetic of ignition (TKI) approach [16] and assuming a constant-volume homogeneous reactor condition. The table of the auto-ignition (AI) times for hydrogen is generated off-line by an automatic numerical procedure, computing the AI times for different levels of pressure, unburned temperature, equivalence ratio, φ, egr and/or water contents. This table is obtained referring to the Konnov kinetic scheme [17]. Once generated, the AI table is inquired and properly interpolated during the calculations. The occurrence of knock phenomenon is recognized in the simulation when the computed Livengood-Wu integral, expressed by equation (6), exceeds an adjustable threshold level, fixed at 0.95 in the present analysis.

$$\int \frac{dt}{\tau_{AI}} < Threshold = 0.95 \tag{8}$$

The in-cylinder heat transfer (gas-to-wall) is replicated by a user sub-model resembling the Woschni equation [18]. A multi-zone approach for the burned zone is utilized to reproduce the NOx formation

[19] within the cylinder. The rate of production of NO is estimated by applying the extended Zeldovich mechanism [20], which allows the thermal NO emissions to be computed without considering the contributions from other source terms.

4. Models validation

The validation of the 1D model related to the single cylinder research engine was performed on an extensive number of experimental points; Table 2 briefly reports the different conditions analysed during the measurements, including the ranges of engine speed, BMEP and equivalence ratio.

Table 2. *Summary of conditions adopted during the Experimental campaign.*

Engine Condition	Range condition	Step
Engine speed, rpm	1500:3000	500
Engine BMEP, bar	3:8	-
Equivalence ratio, Phi	0.4:0.8	0.2

In a first stage, turbulence sub-model is preliminary utilized to replicate the 3D profile of integral length scale (Figure 1a) and then properly tuned to identify a single set of model constants capable to replicate the 3D-derived in-cylinder flow and turbulence variables under motored conditions. After turbulence model tuning, a very good 1D/3D agreement in terms angular evolution of tumble/swirl velocities and of turbulence intensity is obtained for the case at 2000 rpm, as confirmed by Figure 1b and c.

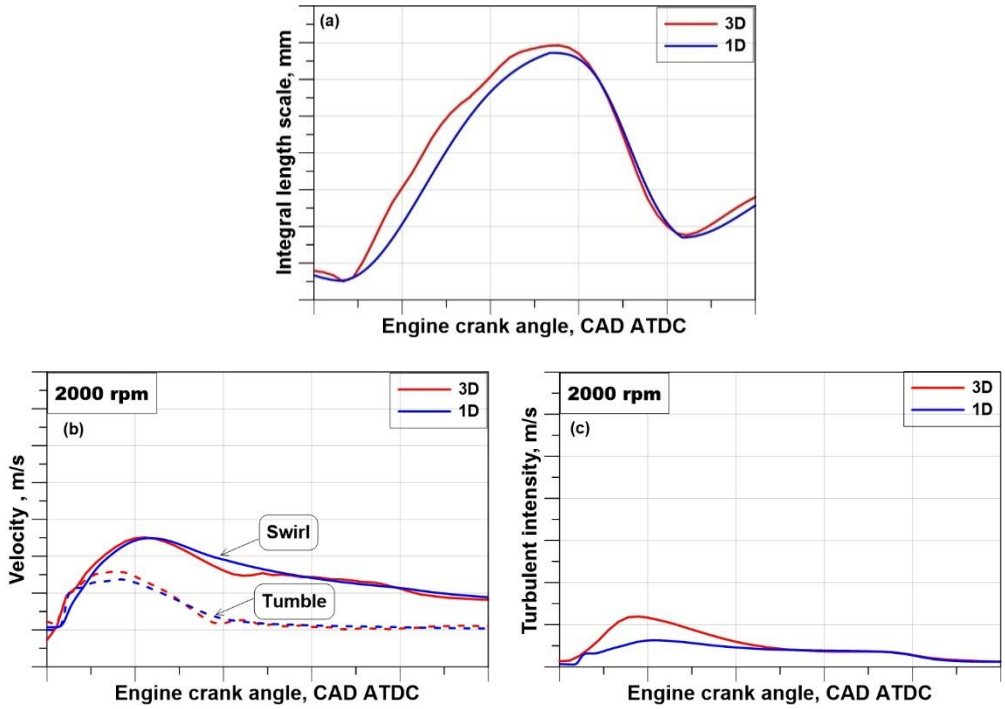

Figure 1. 1D/3D Numerical comparison of integral length scale (a); 1D/3D Numerical/experimental comparison of tumble and swirl velocities at 2000 rpm; (b) 1D/3D Numerical/experimental comparison of turbulence intensity (c) at 2000 rpm.

In a second phase, the engine model is validated under firing conditions to adequately replicate the combustion evolution and the overall performance. To this end, a single set of tuning constants is defined, starting from values obtained for similar engines, and then through a trial and error process the new set of tuning constants is defined, for the combustion sub-model. Figure 2 depicts the outcomes of this validation step, proposing the numerical/experimental comparison in terms of burn rate and pressure cycles (Figure 2a and 2c), and in terms of BMEP and brake thermal efficiency (Figure 2b and 2d).

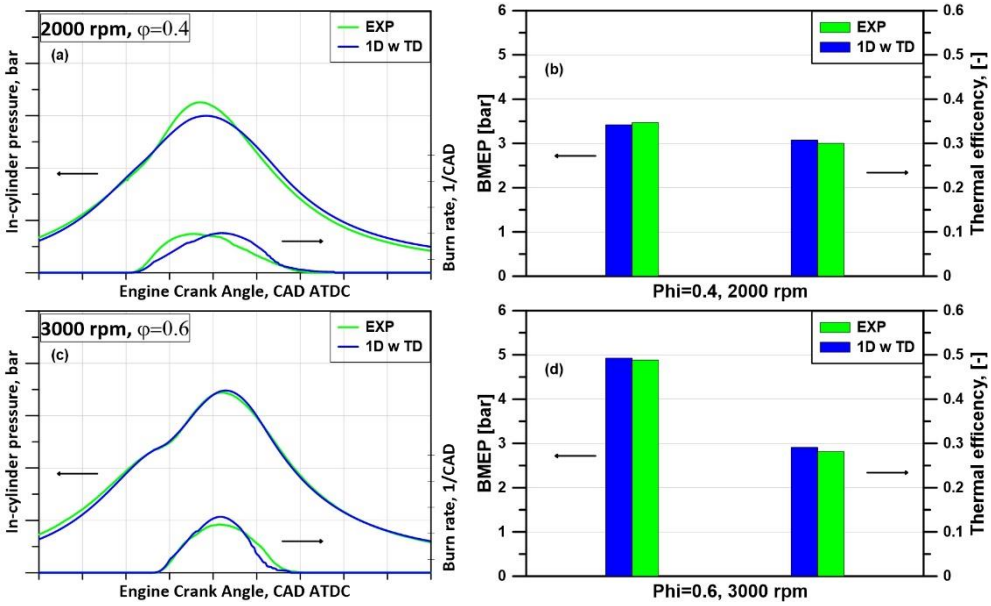

Figure 2. 1D Numerical/experimental comparison of in-cylinder pressure cycles (a), 1D Numerical/experimental comparison of BMEP and brake thermal efficiency (b) at 2000 rpm and ultra-lean mixture (φ=0.4)**.** 1D Numerical/experimental comparison of in-cylinder pressure cycles (c), 1D Numerical/experimental comparison of BMEP and brake thermal efficiency (d) at 3000 rpm and ultra-lean mixture (φ=0.6).

It can be noted from the above reported figures that both combustion evolution and engine performance are reproduced with a good accuracy, even under an ultra-lean air/hydrogen mixture (φ=0.4-0.6). The latter operating condition represents a challenging case to be simulated for a hydrogen engine in a 0D/1D framework. The validated engine model represents an essential pre-requisite for the development of a multi-cylinder hydrogen SI engine, as deeply treated in the next section.

5. Virtual conversion of single cylinder unit to the multi-cylinder engine

Starting from the validated model of the single-cylinder engine (donor engine), a three-cylinder hydrogen SI engine has been developed, assuming the same geometrical characteristics for cylinders and the intake/exhaust valve timings of the donor engine. A proper design for the intake and exhaust sub-systems has been carried out, keeping unchanged some geometrical features, such as the pipes' diameter, and selecting a compromise value for the intake runners length aiming to optimize the volumetric efficiency in the whole engine speed range; this initial design derives from the authors' knowledge gained in the EAGLE research project [21]. The developed multi-cylinder engine has been equipped with a two-stage supercharger system composed by:

1) the low pressure (LP) compressor which is mechanically connected to a Variable geometry turbine (VGT);

2) the high pressure (HP) compressor driven by an electric motor which, in turn, is powered by the battery. The latter is charged with the electric generator (EG) mounted on the engine crankshaft.

The above described engine architecture is schematically plotted in Figure 3 and it is specifically conceived to guarantee engine operation at ultra-lean conditions.

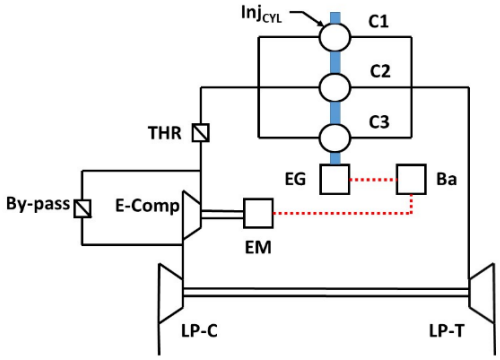

Figure 3. Schematic engine layout of multi-cylinder engine; LP-C: low-pressure compressor; LP-T: low-pressure turbine; E-comp: electric compressor; EM: electric machine; EG: electric generator; Ba: battery; THR: throttle valve; C1/C2/C3: engine cylinders; Inj$_{CYL}$: direct injection; By-pass: valve in the by-pass circuit for E-comp.

6. Methodology description for the multi-cylinder engine

A comprehensive study of the full load curve is carried out using the 1D model of multi-cylinder hydrogen SI engine. In particular, a target full load curve is defined with the speed-related profile and the BMEP values typical for a mid-range engine, as evidenced by the Table 3.

Table 3. BMEP target profile at varying the engine speed

Engine speed, rpm	1000	1500	2000	2500	3000	3500	4000	4500	5000	5500
BMEP, bar	11	13	15	15	15	15	15	15	14	13

In order to achieve the desired BMEP values, while operating the engine with λ=2.0 , the boost pressure required at full load is automatically controlled employing a user-defined strategy for the two-stage boosting system. This means that a proper modulation of boost pressure is realized between LP and HP compressors, while taking into account a maximum allowable level for the boost pressure. Regarding the control strategy of the engine boosting system, a preliminary optimization analysis allowed to define the p_{boost} level provided at the outlet by the LP Compressor by assigning a running line over the performance map. This running line is selected as a compromise between a proper surge margin and a pressure ratio high enough to limit the power absorbed by E-comp. Consequently, the pressure ratio related to the E-comp is straightforwardly identified to match the pre-assigned target BMEP levels. Full load simulations are realized by monitoring the knock occurrence, identifying the knock limited spark advance (KLSA) for each speed/load point; indeed, the numerical knock index is limited to the fixed threshold of AI=0.95.

7. Results Discussion

This section illustrates the results of the numerical analyses carried out for the multi-cylinder SI engine, identifying three main cases structured in the following sub-sections. In a first stage, the performance

and the NOx emissions of the multi-cylinder hydrogen SI engine will be analyzed and then, the effects of compression ratio and port water injection on engine performance and NOx emissions will be studied.

7.1. Performance of multi-cylinder engine

The performance of multi-cylinder engine at full load are initially computed assuming a λ=2 along the points of the target BMEP profile plotted in Figure 4a. Simulations provides the efficiency and BSNOx curves with the engine speed reported in Figure 4b and Figure 4c, respectively. In Figure 4b two efficiency profiles are reported, where the blue one refers to brake thermal efficiency (BTE) neglecting the power absorbed by E-comp. On the other hand, the red curve represents the overall brake thermal efficiency (OBTE) which is shifted below the BTE in the whole speed range. The OBTE can be considered a more consistent engine efficiency, since it takes into account the contribution of power absorbed by the E-comp and then subtracted from the power delivered by engine crankshaft. A peak of OBTE of ~35% is attained at 2000 and 2500 rpm for the full load condition; moving to greater speeds a decreasing efficiency trend can be observed because of increased pumping losses and E-comp power. Despite the absence of a validation for NOx emissions, the predicted BSNOx levels illustrated in Figure 4c is well aligned with those reported in the literature [22] for similar operating conditions.

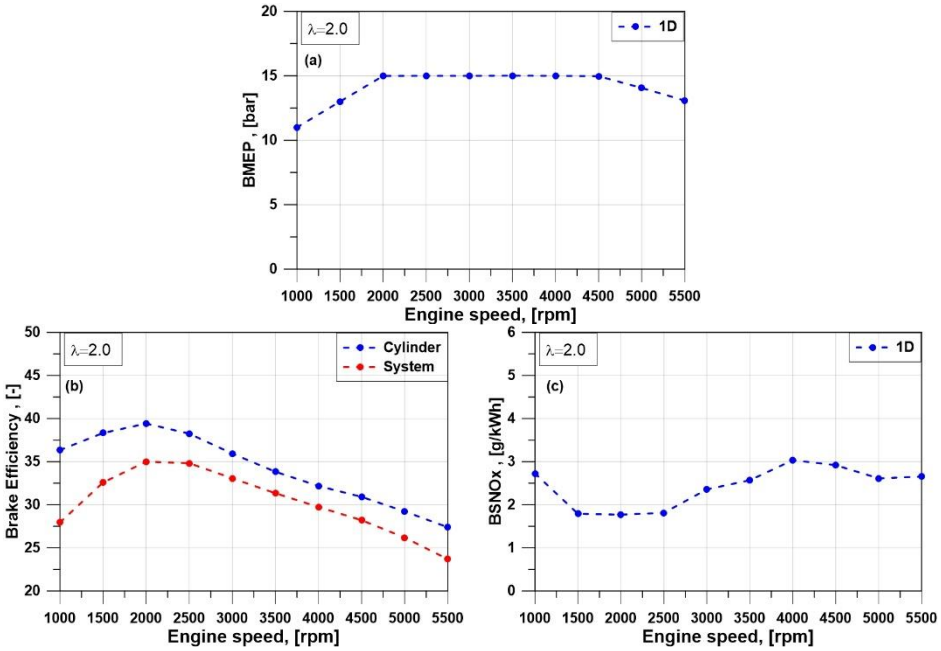

Figure 4. BMEP profile with speed (a); brake efficiency and overall brake efficiency with speed (b); BSNOx curve with speed (c) at full load condition.

The numerical outcomes included in the previous Figure 4 comply with the threshold imposed on the numerical knock index as visible in Figure 5a; therefore the full load points are knock-free and the combustion phasing (MFB_{50}) is equal to the optimum value which, for this engine, corresponds to 10CAD ATDC. In particular, Figure 5a shows that the knock index assumes greater values at high speeds. This can be attributed to the adopted valve timings, which causes a backflow of exhaust gas during the initial intake phase; this phenomenon, in turn, leads to a consequent increase in the temperature of the in-cylinder air/fuel which induces a greater knock tendency.

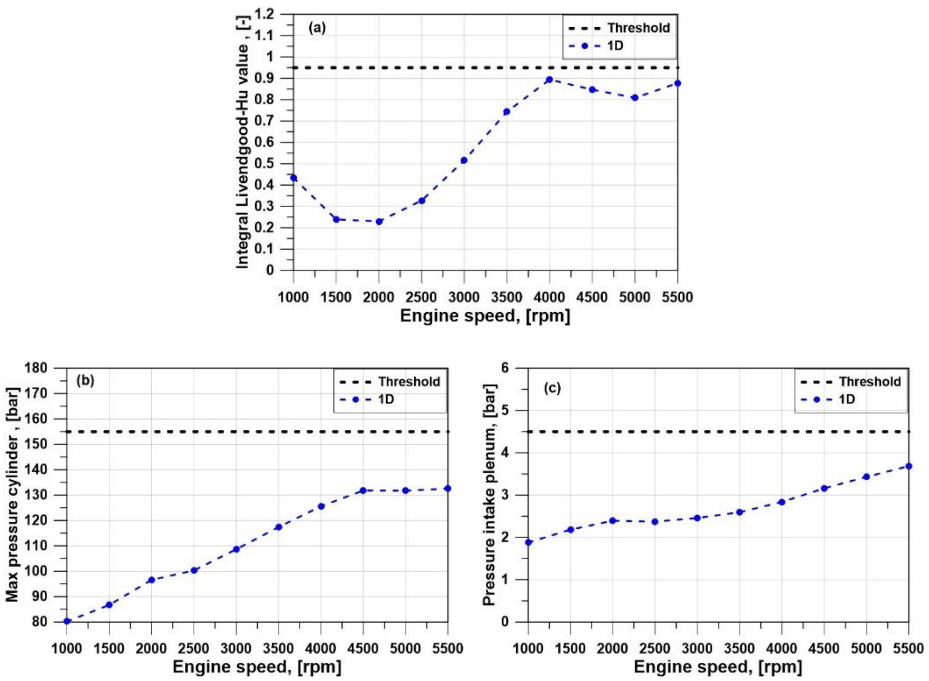

Figure 5. Numerical knock index (a), in-cylinder pressure peak (b) and intake plenum pressure (c) at the full load and different speeds.

The performance and emissions results in Figure 4 also consider additional operating constraints to preserve the mechanical integrity of the engine and its sub-systems. As shown in Figure 5b and Figure 5c, the curves of the in-cylinder pressure peak and intake plenum pressure are well below the corresponding upper bounds. These last are defined basing on a literature analysis [21] and they are set at: 150 bar for the peak pressure and at 4.5 bar for the intake plenum pressure.

7.2. Influence of compression ratio on knock, efficiency and NOx emissions

In order to identify the optimal compression ratio (CR) allowing for an increase in the OBTE levels at full load with λ=2, different geometrical compression ratios, namely 11, 12 and 13 have been analysed. The results related to each CR level are assessed to the outcomes of the initial CR value equal to 10. As illustrated in Figure 6a, the case at CR=11 demonstrates to increase the OBTE along the entire curve compared to the efficiency curve of CR=10. Conversely, the other two cases with greater CR values (CR equal to 12 and 13) exhibit an efficiency deterioration in medium-high speed region due to the knock control; this is confirmed by the delayed combustion phasing (MFB_{50}) from the MBT condition (optimal MFB_{50}=10 CAD ATDC) in Figure 6b. A different behaviour can be noted in low speed zone, where the higher CRs allow to enhance the OBTE values compared to the case at CR=11.
This can be justified by the prevailing effect of increasing the efficiency of the thermodynamic cycle through the greater CR compared to the lower penalty of the retarded combustion phasing induced by the knock control. Indeed, in the low speed region of full load curve the MFB_{50} levels associated to CR=12 and CR=13 are only slightly delayed from the optimal condition (Figure 6b).

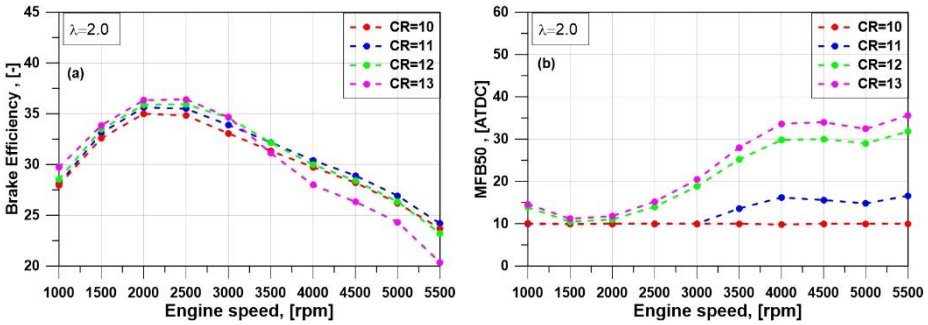

Figure 6. Numerical brake efficiency profile (a) at varying the speed and CR at λ=2; numerical MFB50 profile at varying the speed and CR at λ=2.

Once selected an increased CR level (CR=11) capable to enhance the OBTE all over the full load BMEP curve with respect to the initial CR, a subsequent parametric study by increasing the λ is performed with CR equal to the reference case. This analysis helps to identify the maximum λ value capable of minimizing the NOx emissions while respecting the target BMEP curve. As expected, Figure 7a shows that the lowest NOx emissions are observed in the case of maximum investigated λ, equal to 2.2. However, for the developed multi-cylinder engine, the adoption of λ=2.2 does not allow to match the desired BMEP level at the 5500 rpm, as shown in Figure 7b, this is due to the E-comp failing to provide the level of boost needed. Ultimately, the solution at λ=2.1 is preferred, which guarantees NOx levels only slightly higher than those of λ=2.2 while respecting the BMEP target.

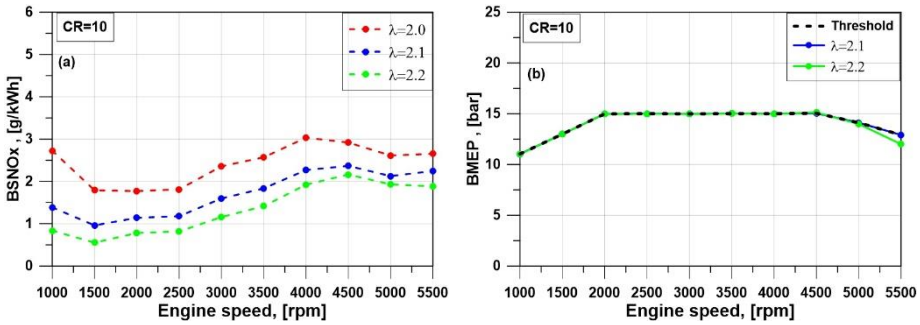

Figure 7. Numerical BSNOx profile (a) with the speed at different λ and at full load; numerical BMEP profile (b) with speed at full load.

7.3. Effect of Water injection on knock and NOx emissions

The last analysis concerns the impact of liquid water injection. A multipoint port water injection (PWI) system is adopted for the examined engine configuration, plotted in Figure 3. This analysis is carried out at 2000 rpm and considering different air/hydrogen mixture ratios (λ levels) and water-to-fuel ratios (defined as the ratio of the fuel mass to the water mass). It is well established that liquid water injection offers significant advantages in terms of knock suppression, due to the high latent heat of water vaporization; in fact, the evaporation of liquid water involves a corresponding heat removal from the in-cylinder fresh mixture which reduces the unburned gas temperatures and, consequently, lowers the knock tendency. This behaviour is illustrated in Figure 8a, showing that as the amount of injected water increases, the numerical knock index decreases for each investigated λ value. Another analysed effect is the impact of water injection on the emission of nitrogen oxides (NOx). As plotted in Figure 8b, the introduction of water injection exerts a relevant reduction in the BSNOx quantities emitted at cylinder-out. The decrease of BSNOx is quite remarkable for the lower λ levels. The λ-related reduction of BSNOx as the W/F ratio increases can be ascribed to the lowering of burned temperatures within the cylinder. Interestingly, the outcomes in Figure 8b highlight that in the cases of λ equal 1.5 and 1.6 the lowering of BSNOx to levels similar to those of ultra-lean mixtures (λ=2.0) requires a W/F ratio greater

than the unity. This implies the adoption of more advanced WI systems (such as high-pressure water direct-injection) and the verification of the effective evaporation of liquid water.

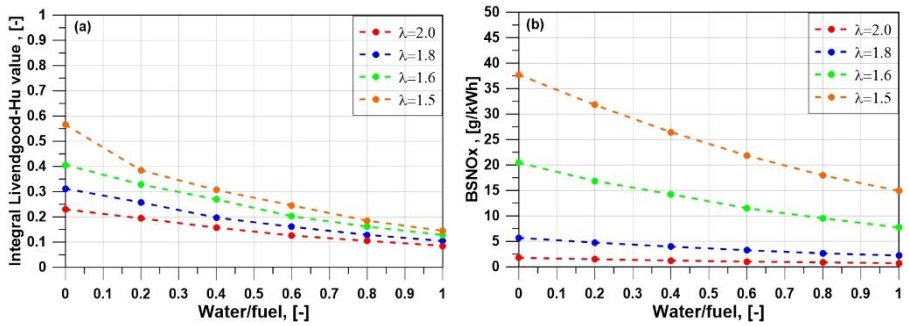

Figure 8. Numerical knock index, LW Integral, (a) at varying the W/F ratio for various λ; numerical BSNOx (b) at varying the W/F ratio for various λ.

8. Conclusion

In this work, a 1D model of a multi-cylinder hydrogen SI engine was developed starting from a validated 1D model of a single-cylinder hydrogen SI engine, with the main aim to forecast and improve the performance and the NOx emissions at full load under lean mixtures. This study also analyzed at the engine full load the effects different compression ratios, λ levels and water/fuel ratios related to a port water injection configuration. The results are summarized as follows:

- multi-cylinder hydrogen engine achieved, in the base case configuration at full load and λ=2, a maximum overall brake efficiency of ~35% and a BSNOx peak of 3g/kWh.
- The study of the different compression ratios at knock borderline showed that the CR maximizing the efficiency in the whole speed range was CR=11; this last led to a maximum efficiency of 35.5%, while the other CRs(CR=12 and CR=13) involved a greater efficiency drop in the medium/high speed zone, due to the knock control, even if they realized higher peak efficiencies (equal to 36.3% and 35.8% for CR=13 and CR=12, respectively).
- The analysis with the different λ levels showed that, for the conceived multi-cylinder engine and boost sharing between HP and LP compressors, the maximum λ value allowing to meet the target full load BMEP is equal to λ=2.1;this last condition also resulted in decreased BSNOx levels at different speeds, lowering the maximum BSNOx at 2.4 g/kWh from the corresponding value at λ=2 equal to 3 g/kWh (percent BSNOx reduction of 20%).
- The water injection investigation was performed at 2000 rpm exploring different water/fuel (W/F) ratios, starting from 0 up to 1 with a of 0.2; water injection analyses was carried out at various λ values: 1.5, 1.6, 1.8 and 2.0; at each λ level, a decreasing trend of NOx was observed as the W/F ratio increases, reaching a maximum percent benefit in the NOx reduction around 60% compared to the dry operation (W/F=0).

References

[1] Seungmoook O.H. et al., “Experimental Investigation of the hydrogen-rich offgas spark ignition engine under various compression ratios”, Energy Conversion and Management, Volume 201, December, N. 112136. doi: 10.1016/j.enconman.2019.112136.
[2] Dhyani V. and Subramanian K.A., “Fundamental characterization of backfire in a hydrogen

fuelled spark ignition engine using CFD and experiments", International Journal of hydrogen Energy, 44 no. 6, 2019: 32254-32270; https://doi.org/10.1016/j.ijhydene.2019.10.077.

[3] Onorati A, Payri R, Vaglieco BM, Agarwal AK, Bae C, Bruneaux G, et al. "The role of hydrogen for future internal combustion engines". International Journal of Engine Research 2022;23:529–40. https://doi.org/10.1177/14680874221081947.

[4] Nande AM, Wallner T, Naber J. "Influence of Water Injection on Performance and Emissions of a Direct-Injection Hydrogen Research Engine". n.d.

[5] Xu P, Ji C, Wang S, Cong X, Ma Z, Tang C, et al. "Effects of direct water injection on engine performance in a hydrogen (H2)-fueled engine at varied amounts of injected water and water injection timing". Int J Hydrogen Energy 2020;45:13523–34. https://doi.org/10.1016/j.ijhydene.2020.03.011.

[6] Maio G, Boberic A, Giarracca L, Aubagnac-Karkar D, Colin O, Duffour F, et al. "Experimental and numerical investigation of a direct injection spark ignition hydrogen engine for heavy-duty applications". Int J Hydrogen Energy 2022;47:29069–84. https://doi.org/10.1016/j.ijhydene.2022.06.184

[7] Luo Y, Wu B, Li Q, Tang X, Yang Z, Wu C, et al. "Experimental and simulation research on the lean combustion characteristics of direct-injection hydrogen engine". Int J Hydrogen Energy 2024;68:398–409. https://doi.org/10.1016/j.ijhydene.2024.04.184

[8] Teodosio L, Berni F, Lanotte A, Malfi E. "1D/3D simulation procedure to investigate the potential of a lean burn hydrogen fuelled engine". ATI 2022.

[9] Bozza F, De Bellis V, Berni F, D'Adamo A, Maresca L. Refinement of a 0D Turbulence Model to Predict Tumble and Turbulent Intensity in SI Engines. Part I: 3D Analyses, 2018. https://doi.org/10.4271/2018-01-0850.

[10] De Bellis V, Bozza F, Fontanesi S, Severi E, Berni F. "Development of a Phenomenological Turbulence Model through a Hierarchical 1D/3D Approach Applied to a VVA Turbocharged Engine". SAE Int J Engines 2016;9:2016-01–0545. https://doi.org/10.4271/2016-01-0545.

[11] De Bellis V, Severi E, Fontanesi S, Bozza F. Hierarchical 1D/3D Approach for the Development of a Turbulent Combustion Model Applied to a VVA Turbocharged Engine. Part II: Combustion Model. Energy Procedia 2014;45:1027–36.

[12] Millo F, Piano A, Rolando L, Accurso F, Gullino F, Roggio S, et al. "Synergetic Application of Zero-, One-, and Three-Dimensional Computational Fluid Dynamics Approaches for Hydrogen-Fuelled Spark Ignition Engine Simulation". SAE Int J Engines 2021;15:03-15-04–0030. https://doi.org/10.4271/03-15-04-0030.

[13] Howarth TL, Hunt EF, Aspden AJ. "Thermodiffusively-unstable lean premixed hydrogen flames: Phenomenology, empirical modelling, and thermal leading points". Combust Flame 2023;253. https://doi.org/10.1016/j.combustflame.2023.112811.

[14] De Bellis V, Piras M, Bozza F, Malfi E, Novella R, Gomez-Soriano J, et al. Development and validation of a phenomenological model for hydrogen fueled PFI internal combustion engines considering Thermo-Diffusive effects on flame speed propagation. Energy Convers Manag 2024;308:118395. https://doi.org/10.1016/j.enconman.2024.118395.

[15] Howarth TL, Aspden AJ. An empirical characteristic scaling model for freely-propagating lean premixed hydrogen flames. Combust Flame 2022;237:111805. https://doi.org/10.1016/j.combustflame.2021.111805.

[16] Bozza F, De Bellis V, Teodosio L. "A Tabulated-Chemistry Approach Applied to a Quasi-Dimensional Combustion Model for a Fast and Accurate Knock Prediction in Spark-Ignition Engines", 2019. https://doi.org/10.4271/2019-01-0471.

[17] Konnov AA. "Yet another kinetic mechanism for hydrogen combustion". Combust Flame 2019;203:14–22. https://doi.org/10.1016/j.combustflame.2019.01.032.

[18] Woschni G. A Universally Applicable Equation for the Instantaneous Heat Transfer Coefficient in the Internal Combustion Engine, 1967. https://doi.org/10.4271/670931.

[19] De Bellis V, Malfi E, Bozza F, KUMAR D, Serrano D, Dulbecco A, et al. "Experimental and 0D

Numerical Investigation of Ultra-Lean Combustion Concept to Improve the Efficiency of SI Engine". SAE Int J Adv Curr Pract Mobil 2021;3:2021-01–0384. https://doi.org/10.4271/2021-01-0384.

[20] LAVOIE GA, HEYWOOD JB, KECK JC." Experimental and Theoretical Study of Nitric Oxide Formation in Internal Combustion Engines". Combustion Science and Technology 1970;1:313–26. https://doi.org/10.1080/00102206908952211.

[21] Bozza F, Tufano D, Malfi E, Teodosio L, Libert C, De Bellis V. "Performance and Emissions of an Advanced Multi-Cylinder SI Engine Operating in Ultra-Lean Conditions". SAE Technical Papers, vol. 2019- September, SAE International; 2019. https://doi.org/10.4271/2019-24-0075

[22] Friedl H, Martin C. "High Efficiency Hydrogen ICE Carbon Free Powertrain for Passenger Car Hybrids and Commercial Vehicles".